Article publicat / *Published paper*:

Karami, Ehsan; Madrigal, Manuel; Gharehpetian, Gevork B.; Rouzbehi, Kumars; Rodríguez, Pedro (2017) Single-phase modeling approach in dynamic harmonic domain. IEEE transactions on power systems, vol.33,iss.1, p.257-267. Doi: 10.1109/TPWRS.2017.2686985

Single-Phase Modeling Approach in Dynamic Harmonic Domain

Ehsan Karami, *Student Member, IEEE*, Manuel Madrigal, *Senior Member, IEEE*, Gevork B. Gharehpetian, *Senior Member, IEEE*, Kumars Rouzbehi, *Senior Member, IEEE*, and Pedro Rodriguez, *Fellow, IEEE*

***Abstract*—In this paper, a frequency-based analytical approach is presented for dynamic analysis of three-phase balanced systems in the presence of harmonic distortion based on single-phase analysis. By providing mathematical foundation, this study proves that a three-phase balanced system (linear or non-linear, supplied by periodic balanced sinusoidal or non-sinusoidal sources) is completely balanced during both transient and steady-state conditions. This is done by utilizing Dynamic Harmonic Domain (DHD) and defining a phase-shift matrix in frequency domain. As the most noteworthy application of the proposed methodology, single-phase modeling approach is put forward. Therefore, during the transient period, one can analyze only one phase of a three-phase balanced system and calculate exact quantities of the other phases without performing extra simulations, which is not possible through time domain. The introduced concept has been applied to different test cases including three-phase transformer inrush current. In addition, the proposed approach has been utilized to obtain a single-phase model of VSC-based power electronic devices for dynamic harmonic analysis, followed by discussion on results.**

***Index Terms*—Dynamic harmonic domain, single-phase modeling, transients analysis, three-phase balanced system.**

I. Introduction

MODERN power systems are complex in nature which leads to several challenges for power system designers and operators. High penetration of power electronics and non-linear loads into electrical power systems can be addressed as a critical issue since analyzing these systems is essential to design and verify the developed energy systems [1]. With the great advancements in the power electronic field and the daily increasing of the non-linear loads, modeling and analysis of harmonic sources have been essential for power quality assessment during both transient and steady states [2], [3].

Dynamic analysis can be performed by means of different methods in both time and frequency domains [4]–[7]. Due to small integration time steps in time domain methods, usually these approaches require long simulation run time even if the steady state response is desired. In comparison to time domain approaches, frequency domain methods use time-varying Fourier series coefficients which are constant or slow-varying quantities under both balanced and unbalanced conditions; therefore, as the main salient feature of these approaches, big time steps can be used during the simulation process.

A review of the literature in this area shows that one of the frequency domain based approaches is dynamic phasor which has been widely used in modeling of electrical power systems such as electrical machines [8], power system dynamics and faults [9], [10], flexible AC transmission systems (FACTS) [11], [12], sub-synchronous resonance [13], unbalanced radial distribution systems [14], and high-voltage direct current (HVDC) systems [15]. In [16], a shifted frequency analysis model which uses dynamic phasor variables instead of instantaneous time variables has been put forward to model synchronous machines for transients around 60 Hz frequency. In [17], application of dynamic phasor concept has been further extended in two major areas. The first was dynamic phasor modeling of frequency varying systems, and the second was dynamic phasor modeling of multi-frequency, multi-generator systems.

Dynamic Harmonic Domain (DHD) is an approach which is basically developed by extension of harmonic domain and dynamic phasor methodologies; it is able to efficiently incorporate dynamic analysis of harmonics during the transient state. This approach employs time-dependent Fourier series and provides the calculation of harmonic evolution in the time domain [18]. Combining the DHD and companion circuit modeling leads to a powerful analytical technique called dynamic companion circuit modeling [19]. The DHD has been successfully applied to FACTS devices, synchronous machines and transmission lines [18]–[21]. An extended harmonic domain model of a wind turbine generator system based on doubly fed induction generator has been presented in [22], which includes both electrical and mechanical subsystems. Moreover, a modified harmonic domain has been proposed in [23] in order to incorporate interharmonics. In [24], a major issue of current implementation of DHD models has been addressed. It is shown that spurious oscillations

Manuscript received July 1, 2016; revised October 23, 2016 and January 13, 2017; accepted March 19, 2017. Date of publication March 24, 2017; date of current version December 20, 2017. Paper no. TPWRS-01000-2016. *(Corresponding author: Ehsan Karami.)*

E. Karami and G. B. Gharehpetian are with the Electrical Engineering Department, Amirkabir University of Technology (Tehran Polytechnic), Tehran 10525, Iran (e-mail:ehsankarami@aut.ac.ir; grptian@aut.ac.ir).

M. Madrigal is with the Instituto Tecnologico de Morelia, Morelia 58120, Mexico (e-mail: manuelmadrigal@ieee.org).

K. Rouzbehi is with the Department of Electrical Engineering, Research Center on Renewable Electrical Energy Systems (SEER), Technical University of Catalonia, Barcelona 08222, Spain (e-mail: Kumars.rouzbehi@upc.edu).

P. Rodriguez is with the Department of Engineering, Loyola University Andalusia, Seville 41014, Spain, and also with the Department of Electrical Engineering, Technical University of Catalonia, Barcelona 08222, Spain (e-mail: prodriguez@uloyola.es).

Color versions of one or more of the figures in this paper are available online at http://ieeexplore.ieee.org.

of individual harmonics appear when including a step change either in input variables or in circuit parameters. However, it has been established that the total response resulted from DHD models, under step changes, is accurate.

An interesting methodology for steady and dynamic states harmonic analysis of power systems has been put forward in [25]. It employs a decomposition framework so that harmonic producing devices are considered as separate subsystems which are solved via the Extended Harmonic Domain (EHD) technique. An approach to reduce a non-linear system in both harmonics and states has been proposed in [26]. The reduced-order model achieves computational savings while preserving accuracy. In the development of the methodology, the authors have taken into account experience and state of the art methods in linear systems theory to yield leaner frequency equivalents than those reported in the power systems literature. Application of DHD for investigating the effect of the source phase angle on harmonic content and time domain response during both transient and steady states has been presented in [27]. As shown, shifting all the sources does not affect the harmonics' magnitude and only harmonics' phase angles are linearly shifted according to their harmonic order.

Steady-state analysis of a three-phase balanced system can be performed based on single-phase representation by calculating each harmonic magnitude and angle for one phase and shifting the results for other phases. From the time domain point of view, however, it is not possible to analyze only one phase of a three-phase balanced system during the transients and obtain exact results of two other phases without solving them directly since exact phase-shift calculation during the transients cannot be done.

This paper aims to establish a foundation for analyzing three-phase balanced systems under dynamic non-sinusoidal conditions based on single-phase modeling approach. In this paper, by providing mathematical foundation, it is shown that in any periodical balanced three-phase system, linear or non-linear, supplied by periodic balanced sinusoidal or non-sinusoidal sources, during transient or steady-state conditions, harmonic *h* in the three-phases, at any time, has the same magnitude, but angles are displaced from one another by $h120^{\circ}$. To such aim, by using Matlab software, a phase-shifting matrix is defined which provides exact phase-shift calculation during both transient and steady states considering each harmonic order; moreover, it has been used to calculate dynamic response of three-phase system based on single-phase analysis. By using the proposed concept of this paper, non-linear loads and three-phase transformers, with different connections, can be described based on single-phase models for dynamic analysis under non-sinusoidal conditions.

II. Dynamic Harmonic Domain

The main idea behind the DHD is that a periodical or quasi-periodic function $x(\tau)$ with period of *T*, can be presented by means of complex Fourier series with time variant coefficients as follows [17], [18]:

$$x(\tau) = \sum_{h=-\infty}^{\infty} X_h(t)\ e^{jh\omega\tau} \quad (1)$$

where, $\tau \epsilon [t, t+T]$, the coefficient $X_h(t)$ is a time-varying complex number and ω is equal to $2\pi/T$. Eq. (1) can be rewritten in the matrix form as follows:

$$x(\tau) = \boldsymbol{E}(\tau)\ \boldsymbol{X}(t) \quad (2)$$

where,

$$\boldsymbol{X}(t) = [\cdots \quad X_{-2}(t) \quad X_{-1}(t) \quad X_0(t) \quad X_1(t) \quad X_2(t) \quad \cdots]^T$$

$$\boldsymbol{E}(\tau) = \left[\cdots \quad e^{-j2\omega\tau} \quad e^{-j\omega\tau} \quad 1 \quad e^{j\omega\tau} \quad e^{j2\omega\tau} \quad \cdots\right]$$

A. State-Space Equation

Considering the general expression of the state-space equation

$$\dot{x}(t) = a(t)\,x(t) + b(t)\,u(t) \quad (3)$$

where, $a(t)$ and $b(t)$ are periodic functions with period of T and the state variable $x(t)$ is in the form of (1). Then, the new state-space equation in the DHD is represented as follows [18]:

$$\dot{\boldsymbol{X}}(t) = (\boldsymbol{A} - \boldsymbol{D})\,\boldsymbol{X}(t) + \boldsymbol{BU} \quad (4)$$

where, $\boldsymbol{D}$ is the differentiation matrix and $\boldsymbol{A}$ and $\boldsymbol{B}$ are Toeplitz matrices formed by the harmonics of $a(t)$ and $b(t)$, respectively [18]. $\boldsymbol{U}$ is a vector formed by the harmonics of $u(t)$. Eq. (4) is the transformation of (3) into the DHD, where the state variable in (3) is $x(t)$ and in (4) are the harmonics of $x(t)$. The steady-state response of (4) is given by the following equation [18]:

$$\boldsymbol{X} = -(\boldsymbol{A} - \boldsymbol{D})^{-1}\boldsymbol{BU} \quad (5)$$

By comparing (3) and (4), it can be observed that the DHD transforms a linear time periodic (LTP) system to a linear time invariant (LTI) system. A particular case of (4) is the steady-state condition given by (5), which is reduced to a set of algebraic equations. Eq. (5) can be used to establish the steady-state condition of the state-space equation.

B. Phase-Shift of Periodic Signals

If a dynamic periodic signal $u(\tau)$ in the form of (1) is time shifted by t_0, i.e. $u(\tau - t_0)$, then we have [27]:

$$u(\tau - t_0) = \sum_{h=-\infty}^{\infty} U_h(t)\ e^{jh\omega(\tau - t_0)}$$
$$= \sum_{h=-\infty}^{\infty} U_h(t)\,e^{-jh\omega t_0}\ e^{jh\omega\tau} \quad (6)$$

This yields a new harmonic coefficient $U_h(t - t_0) = U_h(t)e^{-jh\omega t_0}$, which clearly shows that rotation of the coefficient $U_h(t)$ is the only effect of the frequency domain. This rotation is a linear function of the harmonic *h* which can be interpreted as addition of a linear phase to the original component. By assuming that ωt_0 is equal to α, (6) in the matrix form can be rewritten as follows:

$$u(\tau - t_0) = \boldsymbol{E}(\tau)\,\boldsymbol{SU}(t) \quad (7)$$

where, $\boldsymbol{S}$ is called the phase-shift matrix which is a diagonal matrix of the following form [27]

$$\boldsymbol{S} = diag\left\{\cdots\ e^{j2\alpha}\ e^{j\alpha}\ 1\ e^{-j\alpha}\ e^{-j2\alpha}\ \cdots\right\}$$

According to (7), it can be observed that the harmonics vector of $u(\tau - t_0)$ is given by the following equation:

$$\boldsymbol{U}(t - t_0) = \boldsymbol{S}\,\boldsymbol{U}(t) \tag{8}$$

Eq. (8) presents the harmonics of a phase-shifted function obtained from a non-phase-shifted function. Derivative of $\boldsymbol{U}(t - t_0)$ for dynamic analysis is given by the following equation [27]:

$$\dot{\boldsymbol{U}}(t - t_0) = \boldsymbol{S}\dot{\boldsymbol{U}}(t) \tag{9}$$

According to (9), it can be concluded that the harmonics of the derivative of $u(\tau - t_0)$ is equal to the harmonics of the derivative of $u(\tau)$ multiplied by a phase-shifting matrix. In [27], it is shown that by using properties given in (8) and (9), the dynamic harmonic response of the system to the input $u(\tau - t_0)$ can be directly obtained considering the dynamic harmonic response to input $u(\tau)$ by means of phase-shifting property, and there is no need to perform extra simulation.

III. Harmonics Response in a Three-Phase Balanced System Under Transient and Steady-State Non-Sinusoidal Conditions

Consider a balanced linear or nonlinear three-phase system which is supplied by balanced periodic, non-sinusoidal sources. At any time, during transient or steady-state, the magnitudes of harmonic *h* in three-phases are the same, but their phase angles are displaced from each other by $h120^{\circ}$. These two characteristics are well-known for balanced systems in steady-state, but under the transient period these two conditions have not been addressed so far. This section shows that these two characteristics are also established under transient conditions by employing the DHD. It is worth noting that since the system is balanced, only positive and zero components are present in the waveforms. Moreover, generalized positive sequence component is made only by the first, 5th, 7th … harmonics; and in this case, generalized zero component is only made by multiples of third harmonic [28].

In a general form, assume that each phase contains *n* state variables. For instance, state variables in phase *"a"* can be written as follows:

$$\dot{x}_a(t) = f_a(x_a, x_b, x_c, u_a, u_b, u_c, t) \tag{10}$$

where, f_a can be a general non-linear, time-varying function of state variables (x_a, x_b and x_c with period of *T*), the system inputs (u_a, u_b and u_c), and time (*t*). Moreover, the state variables and inputs in (10) are defined as:

$$x_a(t) = \begin{bmatrix} x_{1a}(t) \\ x_{2a}(t) \\ \vdots \\ x_{na}(t) \end{bmatrix}, u_a(t) = \begin{bmatrix} u_{1a}(t) \\ u_{2a}(t) \\ \vdots \\ u_{ma}(t) \end{bmatrix} \tag{11}$$

where, *m* is the number of input sources. Expanded form of (10) for phase *"a"* is as follows:

$$\begin{aligned}\dot{x}_a(t) &= a_1(t)\,x_a(t) + a_2(t)\,x_b(t) + a_3(t)\,x_c(t) \\ &\quad + b_1(t)\,u_a(t) + b_2(t)\,u_b(t) + b_3(t)\,u_c(t)\end{aligned} \tag{12}$$

here, $a_i(t)$ and $b_i(t)$ (for $i = 1, 2$ and 3) are periodic functions of period *T*. It should be noted that in this representation it is assumed that non-linearities are included by using dependent sources. In a three-phase balanced system, the same equation as shown in (12) can be obtained for phase *"b"* by changing *"a"* to *"b"*, *"b"* to *"c"* and *"c"* to *"a"*. By applying the same transformation to equation of phase *"b"*, equation of phase "*c*" can be achieved. Since the three-phase system is balanced, by applying this transformation the state-space equations of phases *"b"* and *"c"* are as follows:

$$\begin{aligned}\dot{x}_b(t) &= a_1(t)\,x_b(t) + a_2(t)\,x_c(t) + a_3(t)\,x_a(t) \\ &\quad + b_1(t)\,u_b(t) + b_2(t)\,u_c(t) + b_3(t)\,u_a(t)\end{aligned} \tag{13}$$

$$\begin{aligned}\dot{x}_c(t) &= a_1(t)\,x_c(t) + a_2(t)\,x_a(t) + a_3(t)\,x_b(t) + b_1(t)\,u_c(t) \\ &\quad + b_2(t)\,u_a(t) + b_3(t)\,u_b(t)\end{aligned} \tag{14}$$

Transformations of (12), (13) and (14) into the DHD are as follows:

$$\begin{aligned}\dot{\boldsymbol{X}}_a(t) &= (\boldsymbol{A}_1(t) - \boldsymbol{D_d})\boldsymbol{X}_a(t) + \boldsymbol{A}_2(t)\boldsymbol{X}_b(t) + \boldsymbol{A}_3(t)\boldsymbol{X}_c(t) \\ &\quad + \boldsymbol{B}_1(t)\boldsymbol{U}_a(t) + \boldsymbol{B}_2(t)\boldsymbol{U}_b(t) \\ &\quad + \boldsymbol{B}_3(t)\boldsymbol{U}_c(t)\end{aligned} \tag{15}$$

$$\begin{aligned}\dot{\boldsymbol{X}}_b(t) &= (\boldsymbol{A}_1(t) - \boldsymbol{D_d})\,\boldsymbol{X}_b(t) + \boldsymbol{A}_2(t)\,\boldsymbol{X}_c(t) + \boldsymbol{A}_3(t)\,\boldsymbol{X}_a(t) \\ &\quad + \boldsymbol{B}_1(t)\,\boldsymbol{U}_b(t) + \boldsymbol{B}_2(t)\,\boldsymbol{U}_c(t) \\ &\quad + \boldsymbol{B}_3(t)\,\boldsymbol{U}_a(t)\end{aligned} \tag{16}$$

$$\begin{aligned}\dot{\boldsymbol{X}}_c(t) &= (\boldsymbol{A}_1(t) - \boldsymbol{D_d})\,\boldsymbol{X}_c(t) + \boldsymbol{A}_2(t)\,\boldsymbol{X}_a(t) + \boldsymbol{A}_3(t)\,\boldsymbol{X}_b(t) \\ &\quad + \boldsymbol{B}_1(t)\,\boldsymbol{U}_c(t) + \boldsymbol{B}_2(t)\,\boldsymbol{U}_a(t) \\ &\quad + \boldsymbol{B}_3(t)\,\boldsymbol{U}_b(t)\end{aligned} \tag{17}$$

Here,

$$\boldsymbol{D_d} = diag\{\cdots\ \boldsymbol{D}\ \ \boldsymbol{D}\ \ \boldsymbol{D}\ \ \boldsymbol{D}\ \ \boldsymbol{D}\ \cdots\} \tag{18}$$

and $\boldsymbol{A}_i(t)$ and $\boldsymbol{B}_i(t)$ (for $i = 1, 2$ and 3) are Toeplitz matrices formed by the harmonics of $a_i(t)$ and $b_i(t)$, respectively; and $\boldsymbol{U}_j(t)$ (for $j = a$, *b* and *c*) is a vector formed by the harmonics of $u_j(t)$. According to the phase-shifting property, if all the inputs are shifted by α then all the outputs will be shifted by α as well. If both sides of (15) are multiplied by a phase-shifting matrix $\boldsymbol{S_d}$ in which α is equal to -120°, noting that $\boldsymbol{S_d}$ is a diagonal matrix and $\dot{\boldsymbol{S}}_{\boldsymbol{d}}$ is zero, then:

$$\begin{aligned}\boldsymbol{S_d}\dot{\boldsymbol{X}}_a(t) &= (\boldsymbol{A}_1(t) - \boldsymbol{D_d})\,\boldsymbol{S_d}\boldsymbol{X}_a(t) + \boldsymbol{A}_2(t)\,\boldsymbol{S_d}\boldsymbol{X}_b(t) \\ &\quad + \boldsymbol{A}_3(t)\,\boldsymbol{S_d}\boldsymbol{X}_c(t) + \boldsymbol{B}_1(t)\,\boldsymbol{S_d}\boldsymbol{U}_a(t) \\ &\quad + \boldsymbol{B}_2(t)\,\boldsymbol{S_d}\boldsymbol{U}_b(t) + \boldsymbol{B}_3(t)\,\boldsymbol{S_d}\boldsymbol{U}_c(t)\end{aligned} \tag{19}$$

Comparing (16) and (19), it is clear that $\boldsymbol{X}_b(t) = \boldsymbol{S_d}\,\boldsymbol{X}_a(t)$ (according to the phase-shifting property described in [27]) and one can conclude that the dynamic response of phase *"b"* can be directly obtained by dynamic response of phase *"a"*. The same procedure can be followed to obtain dynamic response of phase *"c"*. According to this concept, it is concluded that the dynamic response of a three-phase balanced system can be obtained from the dynamic response of one phase, which is

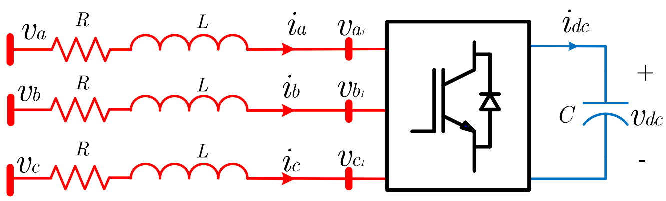

Fig. 1. STATCOM connected to the grid.

not possible through time domain. This principle is used in the following sections.

IV. Single-Phase Model of STATCOM

In this section, the principle of balanced three-phase systems under dynamic non-sinusoidal conditions is used to obtain a single-phase STATCOM model. Fig. 1 shows the three-phase STATCOM circuit scheme with state-space equations as follows [18]:

$$\begin{bmatrix} \frac{di_a}{dt} \\ \frac{di_b}{dt} \\ \frac{di_c}{dt} \\ \frac{dv_{dc}}{dt} \end{bmatrix} = \begin{bmatrix} -R/L & 0 & 0 & -\frac{S_a}{L} \\ 0 & -R/L & 0 & -\frac{S_b}{L} \\ 0 & 0 & -R/L & -\frac{S_c}{L} \\ \frac{S_a}{C} & \frac{S_b}{C} & -\frac{S_c}{C} & 0 \end{bmatrix} \begin{bmatrix} i_a \\ i_b \\ i_c \\ v_{dc} \end{bmatrix} + \frac{1}{L} \begin{bmatrix} v_a \\ v_b \\ v_c \\ 0 \end{bmatrix} \tag{20}$$

where, the switching functions s_a, s_b, and s_c are time-varying functions which represent the operation of the VSC. Eq. (20) has its representation in the DHD by:

$$\begin{bmatrix} \dot{\mathbf{I}}_\mathbf{a} \\ \dot{\mathbf{I}}_\mathbf{b} \\ \dot{\mathbf{I}}_\mathbf{c} \\ \dot{\mathbf{V}}_\mathbf{dc} \end{bmatrix} = \begin{bmatrix} -\frac{R}{L}\mathbf{U}_I - \mathbf{D} & \mathbf{0} & \mathbf{0} & -\frac{1}{L}\boldsymbol{S}_a \\ \mathbf{0} & -\frac{R}{L}\mathbf{U_I} - \mathbf{D} & \mathbf{0} & -\frac{1}{L}\boldsymbol{S}_b \\ \mathbf{0} & \mathbf{0} & -\frac{R}{L}\mathbf{U_I} - \mathbf{D} & -\frac{1}{L}\boldsymbol{S}_c \\ \frac{1}{C}\boldsymbol{S}_a & \frac{1}{C}\boldsymbol{S}_b & \frac{1}{C}\boldsymbol{S}_c & -\boldsymbol{D} \end{bmatrix}$$

$$\times \begin{bmatrix} \mathbf{I_a} \\ \mathbf{I_b} \\ \mathbf{I_c} \\ \mathbf{V_{dc}} \end{bmatrix} + \frac{1}{L} \begin{bmatrix} \mathbf{V_a} \\ \mathbf{V_b} \\ \mathbf{V_c} \\ \mathbf{0} \end{bmatrix} \tag{21}$$

where, $\mathbf{U_I}$ is the identity matrix. From Fig. 1 and (20), the current in the DC-side is given by:

$$C\frac{dv_{dc}}{dt} = s_a\, i_a + s_b i_b + s_c\, i_c = i_{dc} \tag{22}$$

Considering that the system is balanced, then:

$$s_a i_a = \sum_h S_h e^{jh\delta_a} \sum_h I_h e^{jh\delta_a} = \sum_h \sum_k S_k I_{h\,-\,k} e^{jh\delta_a}$$

$$s_b i_b = \sum_h S_h e^{jh\delta_b} \sum_h I_h e^{jh\delta_b} = \sum_h \sum_k S_k I_{h\,-\,k} e^{jh\delta_b}$$

$$s_c i_c = \sum_h S_h e^{jh\delta_c} \sum_h I_h e^{jh\delta_c} = \sum_h \sum_k S_k I_{h\,-\,k} e^{jh\delta_c}$$

Then:

$$s_a i_a + s_b i_b + s_c i_c = \sum_h \sum_k S_k I_{h\,-\,k} \left(e^{jh\delta_a} + e^{jh\delta_b} + e^{jh\delta_c}\right) \tag{23}$$

since $\delta_a = \omega t$, $\delta_b = \omega t - 120^\circ$ and $\delta_c = \omega t + 120^\circ$, (23) can be rewritten as follows:

$$s_a i_a + s_b i_b + s_c i_c = \sum_h \sum_k S_k I_{h-k} e^{jh\omega t}\left(e^0 + e^{-jh120^\circ} + e^{jh120^\circ}\right) \tag{24}$$

Note that $e^0 + e^{-jh120^\circ} + e^{jh120^\circ} = 3$ when $h = 3k$ for $k = 0, 1, \cdots$ and zero otherwise. Consequently:

$$i_{dc} = s_a i_a + s_b i_b + s_c i_c = \sum_{h=0,\pm3,\pm6,\dots} \sum_k 3S_k I_{h\,-\,k} e^{jh\omega t}$$
$$= \sum_h I_{dc_h} e^{jh\omega t} \tag{25}$$

Note that i_{dc} contains the DC-term and triplen harmonics of $s_a i_a$. As an example, the DC-term of i_{dc} is given by $I_{dc_0} = \sum 3S_k I_{-k}$. Now the state-space equations for phase *"a"* and DC side of the STATCOM are given by:

$$\frac{di_a}{dt} = -\frac{R}{L}i_a - \frac{1}{L}s_a v_{dc} + \frac{1}{L}v_a \tag{26}$$

$$\frac{dv_{dc}}{dt} = \frac{1}{C}\, i_{dc} \tag{27}$$

Note that (26) and (27) represent a single-phase model of the STATCOM. These equations in the matrix form are as follows:

$$\begin{bmatrix} \frac{di_a}{dt} \\ \frac{dv_{dc}}{dt} \end{bmatrix} = \begin{bmatrix} -\frac{R}{L} & -\frac{s_a}{L} \\ 0 & 0 \end{bmatrix} \begin{bmatrix} i_a \\ v_{dc} \end{bmatrix} + \begin{bmatrix} \frac{1}{L}v_a \\ \frac{1}{C}i_{dc} \end{bmatrix} \tag{28}$$

Eq. (28) in the DHD is given by:

$$\begin{bmatrix} \dot{\boldsymbol{I}}_\mathbf{a} \\ \dot{\boldsymbol{V}}_\mathbf{dc} \end{bmatrix} = \begin{bmatrix} -\frac{R}{L}\boldsymbol{U}_I - \boldsymbol{D} & -\frac{1}{L}\boldsymbol{S}_a \\ \mathbf{0} & -\boldsymbol{D} \end{bmatrix} \begin{bmatrix} \boldsymbol{I}_a \\ \boldsymbol{V}_{dc} \end{bmatrix} + \begin{bmatrix} \frac{1}{L}\boldsymbol{V}_a \\ \frac{1}{C}\boldsymbol{I}_{dc} \end{bmatrix} \tag{29}$$

here, $\boldsymbol{I}_{dc}$ contains the DC-term and triplen harmonics of $\boldsymbol{S}_a\boldsymbol{I}_a$ and rest are zero. It is worth noting that (29) can be easily obtained by following the procedure that will be described in the next section. However, expanded equations in this section provide a better interpretation.

V. Single-Phase Modeling of Loads and Transformers

Utilizing the proposed concept results in accurate single-phase modeling of different equipment appropriate for dynamic harmonic analysis under non-sinusoidal conditions. Loads and transformers can be connected by different methods, and based on these connections, harmonic content and time domain response during both steady and transient conditions are greatly affected. In order to show the benefits of the proposed method in incorporating phase-shift caused by transformer connection, consider the ideal transformer bank connected in Δ-Y as shown in Fig. 2. Primary and secondary voltages are related as follows:

$$(V_{1a} - V_{1b})/n = V_{2a}/1 \tag{30}$$

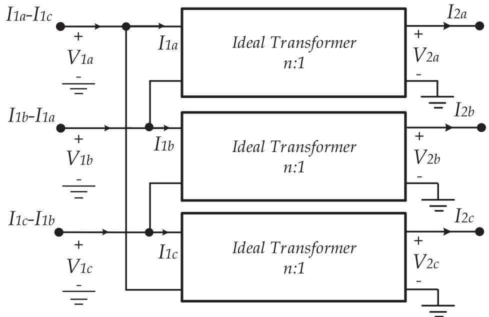

Fig. 2. Transformer connected in Δ-Y.

Since the system is balanced, it is concluded that $V_{1b} = SV_{1a}$; then, (30) can be rewritten as follows:

$$V_{1a} = n \times (U_I - S)^{-1} V_{2a} \tag{31}$$

By following the same procedure and noting that $I_{1c} = S^2\, I_{1a}$, primary side current of phase *"a"* in terms of I_{2a} can be rewritten as $\frac{1}{n} \times (U_I - S^2) I_{2a}$. These equations for voltage and current, provide a connection between primary and secondary sides phase quantities and can be used for nodal analysis in a very efficient manner. By using similar equations for both voltage and current, the proposed concept of this paper can be easily extended to incorporate different loads with different connection styles. This representation for transformers and loads, appropriate for dynamic analysis, is not possible through time domain since an exact phase-shift calculation of harmonic components cannot be performed.

VI. Tests and Results

In order to illustrate the concept of a three-phase balanced system under dynamic non-sinusoidal conditions, three test cases are considered and studied. In the first test case, a three-phase transformer is used to investigate the three-phase inrush currents. In the second test case, the obtained single-phase model for STATCOM in Section IV is used to verify the concept in a more elaborated system. In the third test case, exact single-phase modeling of transformers and loads is included to demonstrate the applicability of the proposed method in analyzing three-phase balanced systems under non-sinusoidal conditions based on the single-phase modeling.

The computer used for the presented simulations is Intel 2.10 GHz central processing unit (CPU) with 8 GB of random access memory (RAM).

A. Transformer Inrush Current

To conform to a three-phase balanced system, consider a three-phase transformer connected in delta-wye and fed with a balanced voltage with a magnitude of 100 V and 60 Hz as shown in Fig. 3. The transformer parameters are the same as reported in [27]. It should be mentioned that in this test case, time step for both DHD and EMTP is equal to 1 μs. Fig. 4 shows the time domain response of current waveform of the inrush current in the transformer by using Electromagnetic Transient Program (EMTP) and DHD which depicts the results are completely

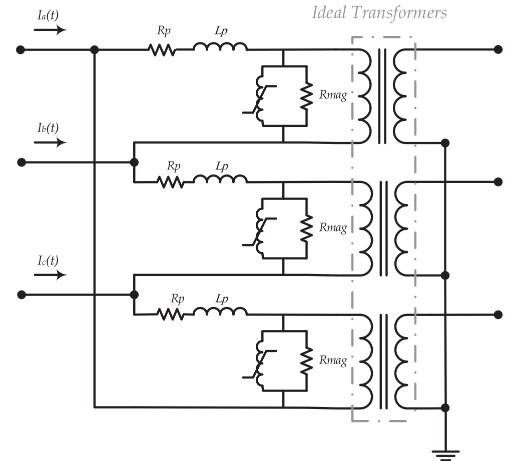

Fig. 3. Three-phase transformer equivalent circuit in delta-wye connection.

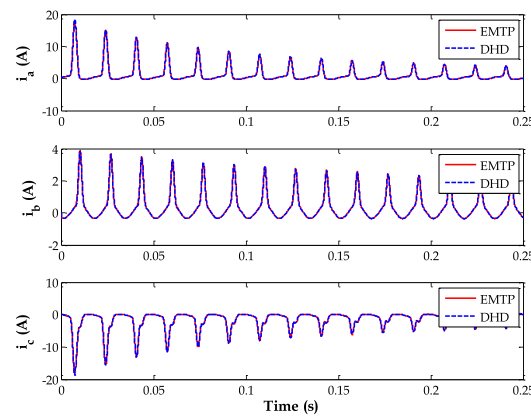

Fig. 4. Inrush currents of three-phases.

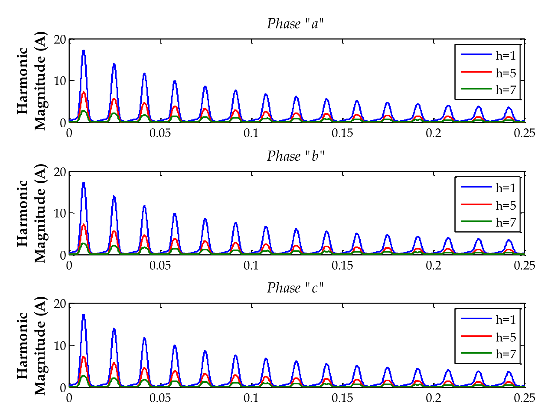

Fig. 5. Harmonic content of inrush currents by using DHD.

matched. However, elapsed time by EMTP is 5.078 s while required time for DHD is 5.139 s. The waveforms are visibly not the same in the three phases and it is not simple to conclude that it is a three-phase balanced system until the transients die out.

Fig. 5 shows the harmonic content of three-phase inrush currents obtained by the DHD. According to Fig. 5, it can be established that the harmonics magnitude in the three phases are identical, which means that three-phase currents have the same THD and RMS. However, this result cannot be observed in

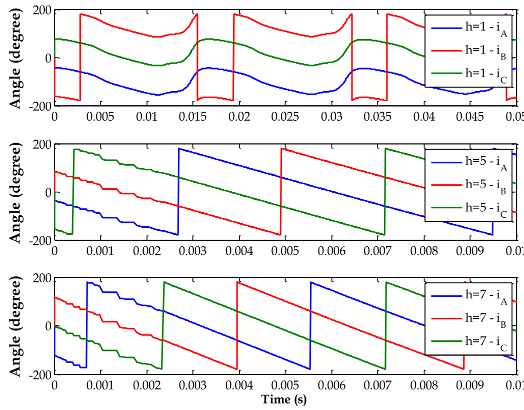

Fig. 6. Angles of harmonic components of three-phase inrush currents by using DHD.

TABLE I
HARMONIC CONTENT OF THREE-PHASE INRUSH CURRENTS AT t = 7.4 ms

Phase	Harmonic Order			Time Domain Response (A)
	$h = 1$	$h = 5$	$h = 7$	
“a”	7.5219 ∢ −121.6423°	3.2074 ∢ −72.8857°	1.3083 ∢ 43.0354°	18.4509
“b”	7.5219 ∢ 118.3577°	3.2074 ∢ 47.1144°	1.3083 ∢ −76.9646°	0.4068
“c”	7.5219 ∢ −1.6424°	3.2074 ∢ 167.1144°	1.3083 ∢ 163.0354°	−18.8577

Fig. 4. In addition, Fig. 6 depicts the phase angles for each harmonic component of the three-phase inrush currents which are obtained through DHD. It should be mentioned that angles are displayed in the range of [−180°, 180°]; hence, when angle reaches −180° or 180°, ±360° is added to the phase angle.

Fig. 6 shows that angles vary in a same way but with a 120° phase-shift regard to a harmonic sequence behavior. Figs. 5 and 6 reveal that despite the significant differences between time-domain waveforms (as shown in Fig. 4), the three-phase inrush currents are balanced during the transient period.

Results of Windowed Fast Fourier Transform (WFFT) are included in Appendix I in order to show that the magnitude of a specific harmonic in each phase is different by using WFFT. In order to show that the time domain responses shown in Fig. 4 for three-phase inrush currents are corresponding to the harmonic content depicted in Figs. 5 and 6, each harmonic response in different phases for t = 7.4 ms (associated to peak value of phase *“a”* shown in Fig. 4) has been presented in Table I. In this table, time domain response of each phase is calculated by (1) as follows:

$$
\begin{aligned}
i_a = & (7.5219\sphericalangle 121.6423^\circ)\, e^{-j\omega_0 \times 0.0074} \\
& + (7.5219\sphericalangle -121.6423^\circ)\, e^{j\omega_0 \times 0.0074} \\
& + (3.2074\sphericalangle 72.8857^\circ)\, e^{-j5\omega_0 \times 0.0074} \\
& + (3.2074\sphericalangle -72.8857^\circ)\, e^{j5\omega_0 \times 0.0074} \\
& + (1.3083\sphericalangle -43.0354^\circ)\, e^{-j7\omega_0 \times 0.0074} \\
& + (1.3083\sphericalangle 43.0354^\circ)\, e^{j7\omega_0 \times 0.0074} = 18.4509A
\end{aligned}
$$

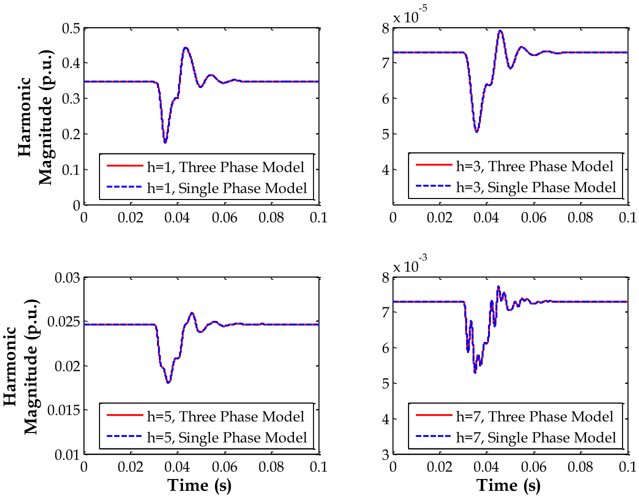

Fig. 7. Harmonic content of phase *“a”* current with PMW technique.

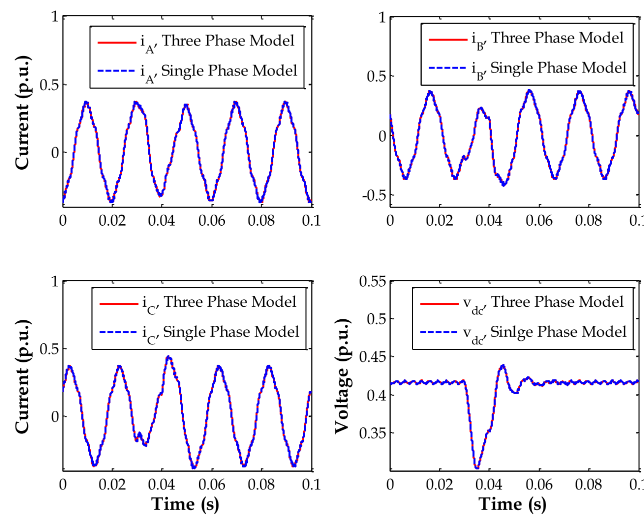

Fig. 8. Waveforms of STATCOM terminal currents and DC-side voltage.

The same procedure can be followed to obtain results of phases *“b”* and *“c”*. According to Table I, it is clear that time domain responses are greatly affected by angles of harmonic components. With these results, it can be concluded that with the dynamic harmonic content of phase *“a”*, waveforms of phases *“b”* and *“c”* can be easily obtained by appropriate phase-shifting according to the harmonic order.

B. Single-Phase Model of STATCOM

In this case, STATCOM of Fig. 1, utilizes a PWM-VSC station with switching frequency of 1 kHz, modulation ratio of unity and with a phase-shift angle $\delta = 5^\circ$ in order to achieve to active and reactive power exchange [18], [29]. In order to provide power factor correction, STATCOM is connected to a local linear load connected in Y with R_L and L_L equal to 0.98 p.u. and 0.785 p.u., respectively. The STATCOM and local load are then connected to the main source with an impedance of 0.001 + j0.031 p.u., and this combination is supplied through a sinusoidal voltage source with magnitude and frequency of 1 p.u. and 50 Hz, respectively.

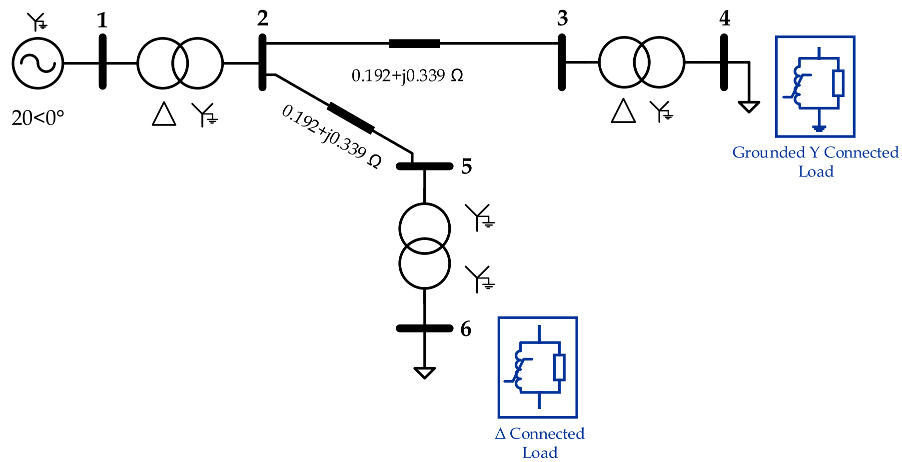

Fig. 9. Single-phase modeling of non-linear components and phase-shifting of transformers in a balanced system.

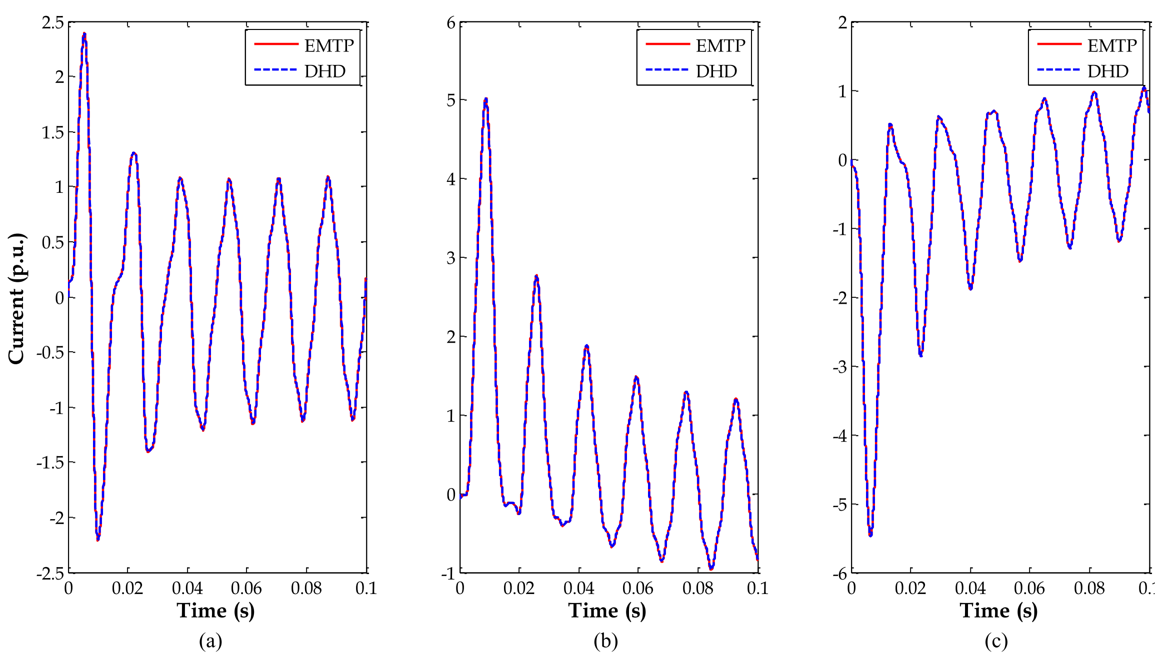

Fig. 10. Current of the source (a) phase *"a"*, (b) phase *"b"* and (c) phase *"c"*.

STATCOM parameters R, L and C are 0.015 p.u., 0.340 p.u. and 4.19 p.u., respectively. For this test system, 50 harmonics are used and steady-state initialization is performed by (5).

In this test system, it is assumed that a disturbance is applied at $t = 30$ ms and lasts for 10 ms during which the magnitude of input voltage source reduces to 80 percent of its value. Fig. 7 shows the harmonic magnitude in the current of phase *"a"* calculated by the single-phase model, using (29), and the three-phase model, using (21). Time domain waveforms of the three-phase STATCOM currents and the DC-side voltage are shown in Fig. 8. Note that current in phase *"b"* and *"c"*, using the single-phase model, are directly obtained based on the proposed approach and the phase-shift matrix. In this case, elapsed time by DHD for three-phase model is 5.211 s, while required time by using DHD for single-phase model is 2.012 s.

C. Single-Phase Model of Loads and Transformers

In this test case, the power system shown in Fig. 9 is used in which two loads are connected to buses 4 and 6. One load is grounded Y and the other one is connected in Δ. In this test system, the transformers are assumed to be ideal. Phase-shifting property is successfully applied to achieve single-phase models for non-linear loads. The same procedure is used to incorporate transformers; see Section V. In this test system, associated equations are expanded for phase *"a"*, which means phase-shifting of transformers is fully considered in the single-phase model for each harmonic component without solving the associated three-phase equations. Current/flux equation of each non-linear load is described by $i_\phi = 0.05\phi + 10^5\phi^5$. Moreover, each non-linear load is in parallel with a linear load with a value of 100 Ω. Further details regarding this test case including

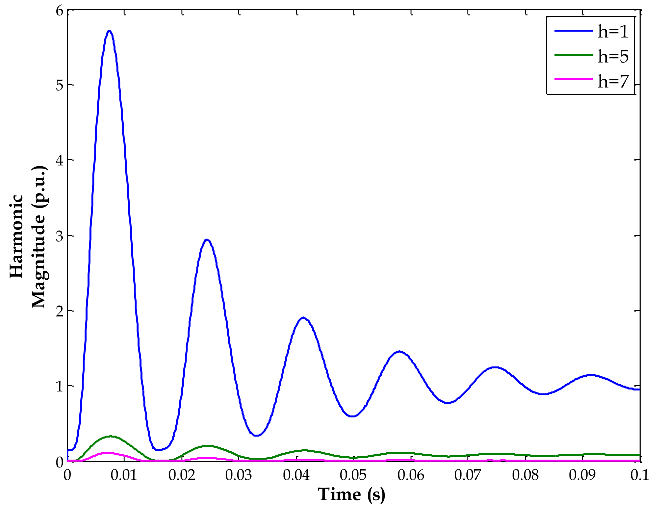

Fig. 11. Harmonic content of source current of phase *"a"*.

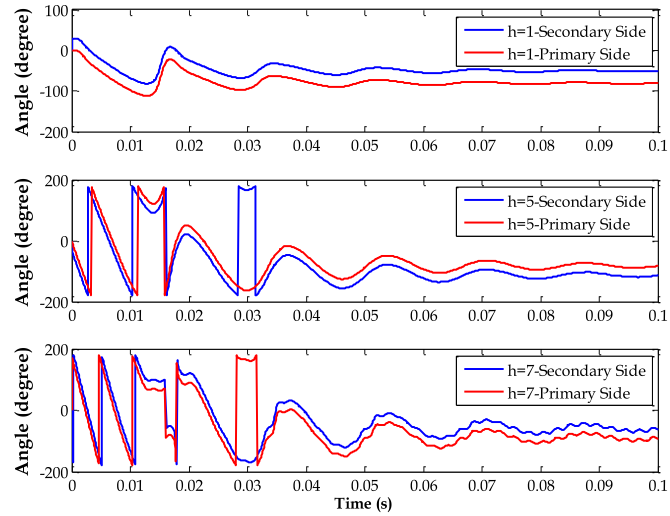

Fig. 12. Harmonic angle of source current of phase *"a"*.

steps required to obtain single-phase equations are provided in Appendix II.

Each transformer is comprised of three ideal transformers with unity transformation. It should be noted that in this test case, all initial conditions are set to zero, and for the sake of simplicity current responses are shown in p.u. with base value of 25 A. Fig. 10(a) shows the phase *"a"* current of the source obtained by both DHD and EMTP. It should be mentioned that in this test case, time step for both DHD and EMTP is equal to 200 μs. Since the system is balanced, phase *"b"* current can be calculated according to the phase-shifting property which is shown in Fig. 10(b). The same procedure can be followed to obtain results of phase *"c"* which is shown in Fig. 10(c). According to Fig. 10, it is clear that results of EMTP and DHD completely matched. However, elapsed time by EMTP is 2.635 s while required time for DHD is 1.013 s. In EMTP, three-phase currents are calculated while DHD solves only one phase and calculates the results of other phases by appropriate phase-shifting during both steady and transient states. Harmonic content of phase *"a"* current at bus 1 is depicted in Fig. 11. As one would expect, there is no third harmonic or its multiples because of the connections of the transformers (Δ) and load connected to bus 6. In order to verify that phase-shifting of transformers is considered in the proposed method, the harmonics' angle of phase *"a"* current in both sides of the transformer which connects buses 1 and 2 are depicted in Fig. 12 where angles are showed in the range of $[-180°, 180°]$. From Fig. 12 which presents the generalized positive sequence, it can be concluded that there is 30° phase-shift according to the harmonic sequence. Therefore, the proposed method easily includes the shifting property of transformers without causing of any complexity. Another property is that non-linear loads (with different connections) are easily described.

Obtained results in different test cases prove that the concept of three-phase balanced system under dynamic non-sinusoidal conditions can be used for exact analyzing of three-phase balanced systems based on single-phase modeling in the presence of harmonic distortion.

VII. Conclusion

This paper explained and discussed the concept of three-phase balanced systems under dynamic non-sinusoidal conditions. In this study, by providing mathematical foundation, it has been proven that despite the significant differences between time domain waveforms, a three–phase balanced system is balanced even during the transient period. By using this concept, one can analyze only one phase of a three-phase balanced system and calculate exact quantities of the other phases during the transient period by appropriate phase-shift. Moreover, using this concept allows obtaining exact single-phase model for both linear and non-linear loads and transformers with different connections appropriate for dynamic harmonic analysis in frequency domain. In addition, phase-shift caused by transformer connection type is easily included based on this single-phase representation. It should be noted that from time domain point of view, since calculating exact phase-shift is not possible, obtaining dynamic single-phase model and computing phase-shift caused by transformer connection is not possible during the transient period. In this paper, the concept of three-phase balanced systems under dynamic non-sinusoidal conditions has been used and applied in order to obtain a dynamic single-phase model for STATCOM, non-linear load and transformer. According to simulation results, it has been proven that the single-phase model was accurately successful to reproduce the dynamic responses in phases *"b"* and *"c"*.

Further research can be conducted to investigate the ability of the proposed approach for real-time applications and transient analyzing of three-phase power systems under unbalanced operation condition in frequency domain.

1) It is worth noting that computational burden is one of the main challenges in real-time studies since they must guarantee the response generation within specified time constraints. The proposed approach substantially reduces the matrix scales than the prevalent DHD methods which can lead to time-efficiency. Therefore, it can be used for real-time applications.

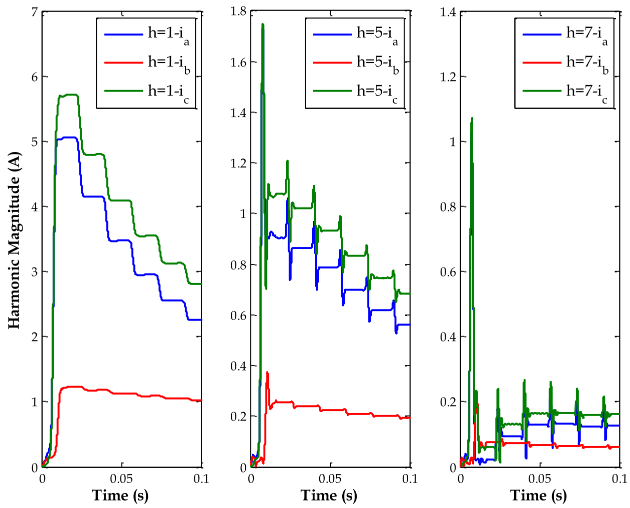

Fig. 13. Harmonic content of inrush currents by using WFFT.

2) Applying the phase-shifting property of harmonics allows calculating exact values of different sequences of generalized symmetrical components under dynamic non-sinusoidal conditions in frequency domain. By combining the generalized symmetrical components along with the concept of a balanced system under dynamic non-sinusoidal conditions (which allows single-phase modeling approach), one can analyze a three-phase power system under unbalanced operation condition.

Appendix I

WFFT allows calculation of harmonic content by sliding a Fast Fourier Transform (FFT) window over a signal. However, fast variations in a time domain waveform are difficult to be detected using WFFT which leads to large errors during the transients since its best performance is limited to stationary waveforms. Fig. 13 depicts the obtained results by using WFFT in order to calculate the harmonic content of the three-phase inrush currents. In this study, for the sake of simplicity, only first, fifth and seventh harmonics are included in Fig. 13. However, WFFT detects all harmonic components in the waveform, such as DC component, second and third harmonics. According to Fig. 13, it is clear that by using WFFT magnitude of a specific harmonic in each phase is different.

Appendix II

Single-phase modeling of loads and transformers appropriate for dynamic analysis in the presence of harmonic distortion has been put forward in Section V. In this section, single-phase state-space equations of test case 3 (see Section VI-C) are presented in more details. It should be noted that in this section, all equations are expanded and shown based on phase *"a"* and S represents a phase-shift matrix in which α is equal to -120°. Moreover, in the following equations, I, V and ψ represent harmonic vectors of i, v and ϕ, respectively.

1) Non-linear load connected to bus 4:

Since at this bus the non-linear load is connected in grounded Y, following equations are easily obtained for current and voltage (I_4 and V_4).

$$\begin{cases} I_4 = \frac{V_4}{R_{L_4}} + I_{\psi_{L_4}} \\ V_4 = D\psi_{L_4} + \frac{d\psi_{L_4}}{dt} \end{cases}$$

Considering the proposed representation for transformers in Section V, Δ side current and voltage (I_3 and V_3) are related to Y side parameters (I_4 and V_4) as follows:

$$\begin{cases} I_3 = \left(U_I - S^2\right) I_4 \\ V_3 = \left(U_I - S\right)^{-1} V_4 \end{cases}$$

1) Non-linear load connected to bus 6:

Fig. 14 depicts detailed representation of this load. According to this figure and by following the procedure explained in Section V, equations that relate phase current and voltage (I_6 and V_6) to load quantities can be written as follows:

$$\begin{cases} I_6 = \left(U_I - S^2\right) \left[\frac{(U_I - S)V_6}{R_{L_6}} + I_{\psi_{L_6}}\right] \\ \left(U_I - S\right) V_6 = D\psi_{L_6} + \frac{d\psi_{L_6}}{dt} \end{cases}$$

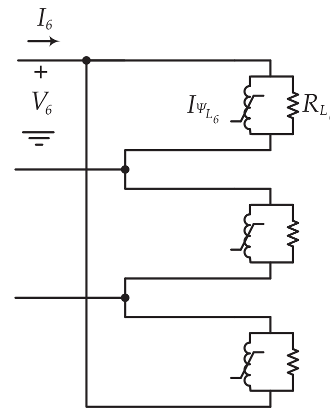

Fig. 14. Non-linear load connected to bus 6.

Since both sides of the transformer that connects busses 5 and 6 are connected in grounded Y, primary side current and voltage (I_5 and V_5) in terms of secondary current and voltage (I_6 and V_6) can be represented as below:

$$\begin{cases} I_5 = I_6 \\ V_5 = V_6 \end{cases}$$

Associated equations for describing transmission lines in the DHD are given by:

$$\begin{cases} V_2 - V_3 = R_{23}\, I_3 + L_{23}\left[\frac{dI_3}{dt} + DI_3\right] \\ V_2 - V_5 = R_{25}\, I_5 + L_{25}\left[\frac{dI_5}{dt} + DI_5\right] \end{cases}$$

According to Fig. 9, it is concluded that current of bus 2 (I_2) is equal to $I_3 + I_5$. Considering the transformer connection, current and voltage of buses 1 (I_1 and V_1) and 2 (I_2 and V_2) are related as given below:

$$\begin{cases} I_1 = \left(U_I - S^2\right) I_2 \\ V_1 = \left(U_I - S\right)^{-1} V_2 \end{cases}$$

Solving the obtained equations in this section for different loads and transformers by using a standard numerical integration method, provides full harmonic analysis based on single-phase modeling. Finally, dynamic response of phases *"b"* and *"c"* can be easily obtained by using phase-shifting property of harmonics in which current and voltage of phase *"a"* are shifted by $\pm 120^{\circ}$.

References

[1] J. Y. Astic, A. Bihain, and M. Jerosolimski, "The mixed Adams-BDF variable step size algorithm to simulate transient and long term phenomena in power systems," *IEEE Trans. Power Syst.*, vol. 9, no. 2, pp. 929–935, May 1994.

[2] E. Acha and M. Madrigal, *Power System Harmonics: Computer Modelling and Analysis*. New York, NY, USA: Wiley, 2001.

[3] S. M. Mazhari, S. M. Kouhsari, and A. Ramirez, "A novel frequency-domain approach for distributed harmonic analysis of multi-area interconnected power systems," *Elect. Power Syst. Res.*, vol. 143, no. 1, pp. 669–681, Feb. 2017.

[4] V. Venkatasubramanian, "Tools for dynamic analysis of the general large power system using time-varying phasors," *Int. J. Elect. Power Energy Syst.*, vol. 16, no. 6, pp. 365–376, Dec. 1994.

[5] S. Henschel, "Analysis of electromagnetic and electromechanical power system transients with dynamic phasors," Ph.D. dissertation, Univ. Brit. Columbia, Vancouver, BC, Canada, 1999.

[6] M. Elizondo, F. Tuffner, and K. Schneider, "Simulation of inrush dynamics for unbalanced distribution systems using dynamic-phasor models," *IEEE Trans. Power Syst.*, vol. 32, no. 1, pp. 633–642, Jan. 2017.

[7] A. M. Stankovic, B. C. Lesieutre, and T. Aydin, "Modeling and analysis of single-phase induction machines with dynamic phasors," *IEEE Trans. Power Syst.*, vol. 14, no. 1, pp. 9–14, Feb. 1999.

[8] A. M. Stankovic, S. R. Sanders, and T. Aydin, "Dynamic phasors in modeling and analysis of unbalanced polyphase AC machines," *IEEE Trans. Energy Convers.*, vol. 17, no. 1, pp. 107–113, Mar. 2002.

[9] A. M. Stankovic and T. Aydin, "Analysis of asymmetrical faults in power systems using dynamic phasors," *IEEE Trans. Power Syst.*, vol. 15, no. 3, pp. 1062–1068, Aug. 2000.

[10] T. Demiray, "Simulation of power system dynamics using dynamic phasor models," Ph.D. dissertation, Swiss Fed. Inst. Technol., Zurich, Switzerland, 2008.

[11] P. Mattavelli, G. C. Verghese, and A. M. Stankovic, "Phasor dynamics of thyristor-controlled series capacitor systems," *IEEE Trans. Power Syst.*, vol. 12, no. 3, pp. 1259–1267, Aug. 1997.

[12] A. M. Stankovic, P. Mattavelli, V. Caliskan, and G. C. Verghese, "Modeling and analysis of FACTS devices with dynamic phasors," in *Proc. 2000 IEEE Power Eng. Soc. Winter Meeting*, 2000, vol. 2, pp. 1440–1446.

[13] M. C. Chudasama and A. M. Kulkarni, "Dynamic phasor analysis of SSR mitigation schemes based on passive phase imbalance," *IEEE Trans. Power Syst.*, vol. 26, no. 3, pp. 1668–1676, Aug. 2011.

[14] Z. Miao, L. Piyasinghe, J. Khazaei, and L. Fan, "Dynamic phasor-based modeling of unbalanced radial distribution systems," *IEEE Trans. Power Syst.*, vol. 30, no. 6, pp. 3102–3109, Nov. 2015.

[15] H. Zhu, Z. Cai, H. Liu, Q. Qi, and Y. Ni, "Hybrid-model transient stability simulation using dynamic phasors based HVDC system model," *Elect. Power Syst. Res.*, vol. 76, pp. 582–591, Apr. 2006.

[16] P. Zhang, J. R. Marti, and H. W. Dommel, "Synchronous machine modelling based on shifted frequency analysis," *IEEE Trans. Power Syst.*, vol. 22, no. 3, pp. 1139–1147, Aug. 2007.

[17] T. Yang, S. Bozkho, J. Le-Peuvedic, G. Asher, and C. Hill, "Dynamic phasor modeling of multi-generator variable frequency electrical power systems," *IEEE Trans. Power Syst.*, vol. 31, no. 1, pp. 563–571, Feb. 2015.

[18] J. J. Rico, M. Madrigal, and E. Acha, "Dynamic harmonic evolution using the extended harmonic domain," *IEEE Trans. Power Del.*, vol. 18, no. 2, pp. 587–594, Apr. 2003.

[19] H. García, M. Madrigal, B. Vyakaranam, R. Rarick, and F. E. Villaseca, "Dynamic companion harmonic circuit models for analysis of power systems with embedded power electronics devices," *Elect. Power Syst. Res.*, vol. 81, no. 2, pp. 340–346, Feb. 2011.

[20] B. Vyakaranam and F. E. Villaseca, "Dynamic modeling and analysis of generalized unified power flow controller," *Elect. Power Syst. Res.*, vol. 106, pp. 1–11, Jan. 2014.

[21] J. J. Chavez, A. Ramirez, and V. Dinavahi, "Dynamic harmonic domain modelling of synchronous machine and transmission line interface," *IET Gener. Transm. Distrib.*, vol. 5, no. 9, pp. 912–920, Sep. 2011.

[22] U. Vargas and A. Ramirez, "Extended harmonic domain model of a wind turbine generator for harmonic transient analysis," *IEEE Trans. Power Del.*, vol. 31, no. 3, pp. 1360–1368, Jun. 2016.

[23] A. Ramirez, "The modified harmonic domain: Interharmonics," *IEEE Trans. Power Del.*, vol. 26, no. 1, pp. 235–241, Jan. 2011.

[24] F. Yahyaie and P. W. Lehn, "On dynamic evaluation of harmonics using generalized averaging techniques," *IEEE Trans. Power Syst.*, vol. 30, no. 5, pp. 2216–2224, Sep. 2015.

[25] S. M. Mazhari, S. M. Kouhsari, A. Ramirez, and E. Karami, "Interfacing transient stability and extended harmonic domain for dynamic harmonic analysis of power systems," *IET Gener. Transm. Distrib.*, vol. 10, no. 11, pp. 2720–2730, Aug. 2016.

[26] A. Ramirez and J. J. Rico, "Harmonic/state model order reduction of nonlinear networks," *IEEE Trans. Power Del.*, vol. 31, no. 3, pp. 1379–1387, Jun. 2016.

[27] E. Karami, G. B. Gharehpetian, and M. Madrigal, "A step forward in application of dynamic harmonic domain: Phase shifting property of harmonics," *IEEE Trans. Power Del.*, vol. 32, no. 1, pp. 219–225, Feb. 2017.

[28] P. Tenti, J. L. Willems, P. Mattavelli, and E. Tedeschi, "Generalized symmetrical components for periodic non-sinusoidal three-phase signals," *Elect. Power Qual. Utilization*, vol. XIII, no. 1, pp. 9–15, 2007.

[29] M. Madrigal, "Modelling of power electronics controllers for harmonic analysis in power systems," Ph.D. dissertation, Univ. Glasgow, Glasgow, U.K., 2001.

Ehsan Karami was born in Kermanshah, Iran, in September 1991. He received the M.Sc. degree in electrical engineering from Amirkabir University of Technology (Tehran Polytechnic), Tehran, Iran, in 2015.

He is currently in the Electrical Engineering Department, Amirkabir University of Technology. He is an Engineer in Iran and has working experience with transmission and distribution utilities, oil and gas companies, and research institutes, including several polymer companies and Niroo Research Institute. His main areas of research are power system harmonics and power quality, transients in power systems, and FACTS devices.

Manuel Madrigal (SM'96) received the Graduation degree from the Instituto Tecnologico de Morelia, Morelia, Mexico, in 1993, the M.Sc. degree in electrical engineering from the Universidad Autonoma de Nuevo Leon, San Nicolás, Mexico, in 1996, and the Ph.D. degree from the University of Glasgow, Glasgow, U.K., in 2001. Since 1996, he has been a Graduate Research Professor in the Instituto Tecnologico de Morelia. His research interests include power quality and harmonic analysis in power systems.

Gevork B. Gharehpetian (SM'08) received the B.S., M.S., and Ph.D. degrees in electrical engineering, all with First Class Hons., from Tabriz University, Tabriz, Iran, Amirkabir University of Technology (AUT), Tehran, Iran, and Tehran University, Tehran, Iran, respectively, in 1987, 1989, and 1996, respectively.

As a Ph.D. student, he received scholarship from DAAD (German Academic Exchange Service) from 1993 to 1996, and he was in the High Voltage Institute of RWTH Aachen, Aachen, Germany. He was an Assistant Professor at AUT from 1997 to 2003, an Associate Professor from 2004 to 2007, and has been a Professor since 2007. He is a member of the power engineering group of AUT which has been selected as a Center of Excellence on Power Systems in Iran since 2001. He was selected by the Ministry of Higher Education as the Distinguished Professor of Iran and by Iranian Association of Electrical and Electronics Engineers (IAEEE) as the Distinguished Researcher of Iran and was awarded the National Prize in 2008 and 2010, respectively. Based on the ISI Web of Science database (2005–2015), he is among the world's top 1% elite scientists according to Essential Science Indicators (ESI) ranking system. He is the author of more than 1000 journals and conference papers. His teaching and research interests include smart grid, microgrids, FACTS and HVDC systems, and monitoring of power transformers and its transients.

Prof. Gharehpetian is a distinguished member of IAEEE and a member of the central board of IAEEE. Since 2004, he has been the Editor-in-Chief of the *Journal of IAEEE*.

Kumars Rouzbehi (S'13–M'16–SM'16) received the Ph.D. degree in electric energy systems from the Technical University of Catalonia, Barcelona, Spain, in 2016.

Prior to his Ph.D. program, he was with the Faculty of Electrical Engineering, Islamic Azad University (IAU), from 2004 to 2011, where he became the Director of the Department of Electrical Engineering. In parallel with teaching and research at IAU, he was the CEO of Khorasan Electric and Electronics Industries Researches Company from 2004 to 2010. He holds a patent in AC grid synchronization of voltage source converters and has authored and coauthored several technical books, journal papers, and technical conference proceedings.

Dr. Rouzbehi has been a member of the *Amvaje-e-bartar* (an Iranian journal of electrical engineering) Policy Making Committee and has served as an Editor since 2006. He received the Second Best Paper Award 2015 from the IEEE Power Electronics Society from the IEEE JOURNAL OF EMERGING AND SELECTED TOPICS ON POWER ELECTRONICS. He has been a TPC Member of the International Conference on Electronic, Communication, Control and Power Engineering (IEEE-ECCP) since 2014 and a Scientific Board Member of the (IEA) International Conference on Technology and Energy Management since 2015.

Pedro Rodriguez (F'13) received the M.Sc. and Ph.D. degrees in electrical engineering from the Technical University of Catalunya (UPC), Barcelona, Spain.

In 1990, he joined the UPC, where he became the Director of the Research Center on Renewable Electrical Energy Systems (SEER) and still collaborates with the UPC as a Visiting Professor. In 2005, he was a Visiting Researcher with the Center for Power Electronics Systems, Virginia Tech. In 2006 and 2007, he was a Postdoctoral Researcher in the Department of Energy Technology, Aalborg University (AAU). From 2007 to 2011, he was a co-supervisor of the Vestas Power Program at the AAU. From 2011 to 2017, he was the Director of Technology on the area of power systems in Abengoa Research, Spain. Since 2017, he has been with the Loyola University Andalucia, Seville, Spain, as a Full Professor. He has coauthored one Wiley-IEEE book, more than 80 papers in ISI technical journals, and around 250 papers in conference proceedings. He is the holder of 14 licensed patents. His research interests include distributed power systems, flexible transmission systems, and power conversion.

Dr. Rodriguez is an IEEE Fellow for his contributions in the control of distributed generation, an Associate Editor of the IEEE TRANSACTION ON POWER ELECTRONICS and a member of the Sustainability and Renewable Energy Committee of the IEEE Industry Application Society and the Renewable Energy Systems Technical Committee of the Industrial Electronics Society.